

Micro check valves for integration into polymeric microfluidic devices

Nam-Trung Nguyen¹, Thai-Quang Truong¹, Kok-Keong Wong¹,
Soon-Seng Ho² and Cassandra Lee-Ngo Low²

¹ School of Mechanical and Production Engineering, Nanyang Technological University,
50 Nanyang Avenue, Singapore 639798

² School of Electronics and Electrical Engineering, Singapore Polytechnic, 500 Dover Road,
Singapore 139651

E-mail: mntnguyen@ntu.edu.sg

Received 12 May 2003, in final form 30 July 2003

Published 18 August 2003

Online at stacks.iop.org/JMM/14/69

Abstract

In this paper we describe the design, simulation, fabrication and characterization of micro check valves suitable for integration into polymeric microfluidic devices such as micropumps or test cartridges for biomedical analysis. The valves are fabricated by a polymeric surface micromachining process, which utilizes SU-8 as the functional material. The devices are assembled with the lamination technique. A micro check valve consists of three layers: an inlet layer, a valve layer and an outlet layer. The valve is a disc with a diameter of 1 mm. The disc is suspended on folded beams, which act as valve springs. Both valve disc and springs are fabricated in a 100 μm SU-8 layer. The valves prove a clear flow rectification function. Relatively low pressure is required for opening the valve. The valves were tested and characterized with water. One of the valves is successfully integrated into a polymeric micropump. These valves prove the facile and reliable lamination technology for the fabrication of complex polymeric microfluidic devices for biomedical analysis.

1. Introduction

Recently, microfluidics has emerged as an exciting research field with many applications [1]. One of the main growth thrusts of microfluidics is microfluidic analysis devices, the so-called lab-on-a-chip. A number of chemical and biochemical assays have been successfully implemented. Applications such as DNA sequencing [2], antigen detection [3] and high-throughput genotyping [4] have been implemented in microfluidic platforms. Many of these devices have been fabricated in glass and silicon, which require complex fabrication processes and pose possible problems with biocompatibility. Furthermore, the relatively large size of microfluidic systems utilize large silicon surfaces that makes a microfluidic chip more expensive. Efforts have been made to fabricate polymeric microfluidic devices. The polymeric lab-on-a-chip has the potential for low cost and high biocompatibility. Automated genotyping including purification, amplification and hybridization has been implemented in a polymeric device [5]. Polymer analysis

cartridges for blood analysis are commercially available [6]. Another polymer cartridge for automated pathogen detection has been demonstrated [7]. An elastomer cartridge has been developed for multiplex detection of nucleic acid sequences [8]. The latter cartridge has an integrated diffuser/nozzle pump for delivering fluids. Another concept combines glass and elastomer to realize a peristaltic micropump with pneumatic actuation [9]. An elastomer cartridge has been used as the interconnection solution for hybrid integration of off-the-shelf components, but no fluidic component was integrated in this platform [10].

The recent emergence of polymeric microfluidic cartridges shows the trend of low-cost disposable non-silicon microfluidic devices. The need for cheap polymeric devices has led to the development of new fabrication technologies. Our technological approach is to fabricate size-critical components with the conventional microtechnique of lithography, while large structures such as channels can be fabricated in cheaper ways such as moulding, hot embossing or laser machining. Furthermore, the polymeric technology

can also include packaging techniques such as layer-by-layer lamination in order to solve the relatively costly interconnection problem. We have developed a technology which combines lithography of thick-film resists such as SU-8 with cheaper materials and technology such as laser cutting of polymethylmethacrylate (PMMA). This approach was proven by the realization of a number of microfluidic devices such as microchannels, micromixers, micro check valves, micro Tesla valves, micropumps and passive microflow controllers. In this paper we focus on the development of SU-8 micro check valves. Although the devices are stand-alone, the integration in a complex microfluidic cartridge is feasible.

The passive valve is one of the most important microfluidic components. Several micro check valve designs have been realized in the past. Although they differ in shape and material, all check valves have the same function of flow rectification. Micro check valves can be categorized by their forms such as ring mesa, cantilever, disc, V-shape and membrane [11]. Micro check valves can be used as stand-alone microfluidic components. However, their most popular application is the use in a reciprocating micropump. Varieties of micro check valves have been integrated in reciprocating micropumps [1]. The requirements on micro check valves for this application are low leakage in the reverse direction and low spring constant. Most of the silicon micropumps have check valves made of silicon and metals, which are relatively stiff [12]. Furthermore, these check valves have hard sealing surfaces and may cause large leakage in the reverse direction.

Polymeric check valves offer unique advantages over their silicon and metal counterparts. With a Young's modulus of two orders less than that of silicon and metals, polymeric microvalves have a much lower spring constant allowing us to open the valve with much less pressure. The soft sealing surface allows a zero-leakage design. A number of polymeric valves have been fabricated in different materials such as polyimide [13], polysulfone (PSU) [14], polyester [15] and recently polydimethylsiloxane (PDMS) [9]. Many of the valves have been fabricated on glass or silicon substrates, thus are not fully polymeric and may have chemical compatibility problems in lab-on-a-chip applications.

In this paper we offer a new alternative to making fully polymeric microvalves. We use SU-8 as the functional material which is structured by polymeric surface micromachining. SU-8 is coated over a sacrificial layer on a silicon substrate. Etching away the sacrificial layer releases the freely movable SU-8 structures. This SU-8 layer is then considered as one functional layer in the subsequent multilayer lamination. Other layers are made of laser-machined PMMA sheets and double-sided adhesive tapes.

Here we present the design, fabrication and characterization of the SU-8 micro check valves. The successful operation of the valves facilitates the development of fully polymeric analysis cartridges for biomedical applications.

2. Design and simulation

The check valve is designed as a disc suspended on N folded beams, which work as valve springs. The folded beams can be

considered as springs connected in parallel. Thus, the force at each beam is

$$F = \frac{F_0}{N} = \frac{p\pi r_d^2}{N} \quad (1)$$

where p is the pressure applied on the valve disc and r_d is the radius of the valve disc. Each folded beam can be seen as connected beam segments or springs connected in serial. The total deflection of the valve disc is the sum of all the deflections of the beam segments:

$$\delta = \sum_{i=1}^N \delta_i. \quad (2)$$

With a beam thickness of 100 μm , the deflections can be assumed as small enough to be in the linear range. Thus, linear beam equations are adequate for the analytical analysis. The deflection of each beam segment can be modelled as a straight beam, which is fixed at one end and guided at the other end [16]:

$$\delta_i = \frac{FL_i^3}{12EI}. \quad (3)$$

Here, F is the force at the guided end, L_i is the length of the beam segment, E is the Young's modulus of the beam material and I is the moment of inertia

$$I = \frac{wh^3}{12} \quad (4)$$

where w is the width and h is the thickness of the beam. Thus, the total spring constant of the valve is calculated as [17]

$$k_{\text{Valve}} = \frac{F_0}{\delta} = \frac{N}{\sum_{i=1}^N \frac{L_i^3}{12EI}}. \quad (5)$$

The different designs investigated in this paper are depicted in figure 1. The curved segments of the arms can be modelled analytically as a beam with a fixed end and a guided end [17]. The smaller the curvature angle and the larger the radius of curvature of the segments, the better this assumption is. With the space constraint, the length of the curved segments can be changed by varying the angle α .

While valve design 5 only has one suspension arm, valve designs 2, 3, 4 and 6 have two suspension arms. The advantage of the small number of arms ($N = 1$ and $N = 2$) is low spring constant. However, rotation around the suspension axis may cause unexpected behaviour of the disc displacement. With more than three arms $N \geq 3$, the valve disc can move parallel to its base plane with no rotation. The designs with three or more arms are called ortho-planar springs [17]. The advantage of ortho-planar design is the stable parallel out-of-plane deflection. The disadvantage is much stiffer total spring constant, because the suspension arms can be considered as springs connected in parallel.

Figure 2 shows the simulation results with ANSYS using the element type SHELL 63. The valve disc in this model is loaded with a pressure p . The resulting deflection δ of the disc is used for calculation of the spring constant of the valve:

$$k_{\text{Valve}} = \frac{F_0}{\delta} = \frac{p\pi r_d^2}{\delta}. \quad (6)$$

Table 1 compares the spring constants of the different valve designs using the analytical model (5) and the numerical simulation (6). The results show that the analytical

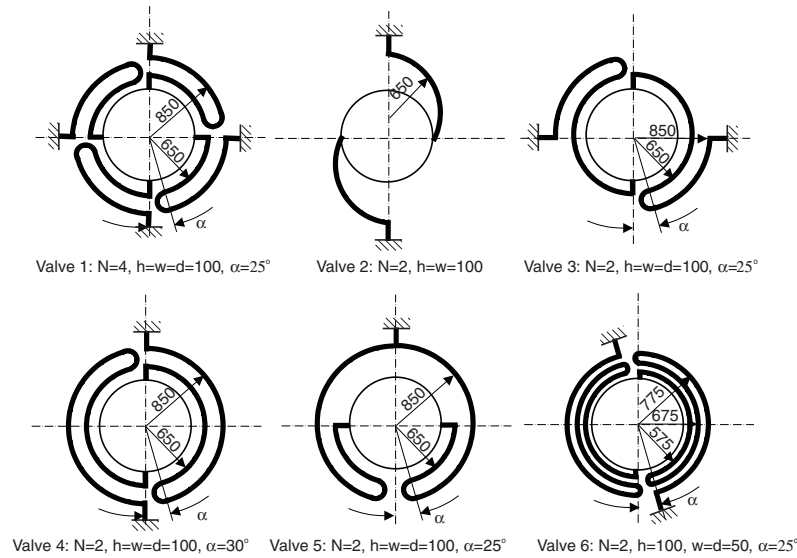


Figure 1. Different valve designs and their geometry parameters (in micrometres): h , layer thickness; w , beam width; d , the gap between folded beam sections. All valve discs have a diameter of 1 mm.

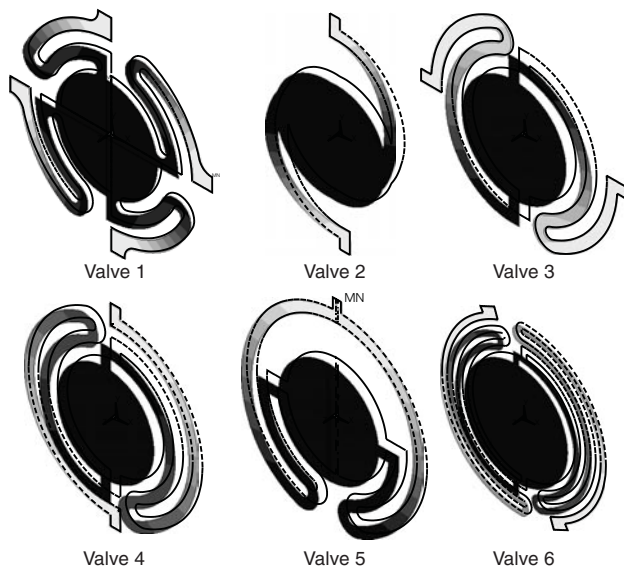


Figure 2. Deflection of different valves with pressure load on the valve discs (numerical simulation with ANSYS).

Table 1. Spring constants of the different valve designs (in N m^{-1} , calculated for a Young's modulus of $4.02 \times 10^9 \text{ Pa}$ [18]).

Calculation	Valve 1	Valve 2	Valve 3	Valve 4	Valve 5	Valve 6
Analytical	807	490	127	57	64	21
Simulation	613	499	95	65	59	31

model can only be used for rough estimation of the spring constants.

The prediction of the behaviour of the check valve requires a coupled fluid–structural simulation. The usual approach is to run the structural and flow analyses separately with two different solvers [19, 20]. The deflection of the valve is used

for shaping the grid of the fluid domain. In turn, the pressure distribution from the flow analysis is used as the boundary condition for the structural analysis. The multiphysics feature of ANSYS also allows this coupling approach. However, this simulation approach is very time-consuming. For complicated structures such as our valve designs, a complex three-dimensional model is necessary for the simulation. The three-dimensional coupled fluid–structural simulation is even more complex and time-consuming.

Because the valve disc in our case is assumed to move parallel to its surface, the behaviour of the valve displacement is straightforward. A linear displacement with a constant spring constant can be calculated. Only one structural analysis needs to be carried out for determining the spring constant. This stiffness can then be used for a semi-analytical coupled simulation described next.

The coupling was realized in an iteration loop written as a macro script in the ANSYS batch file. First, the flow analysis was carried out for an initial gap between the valve disc and the inlet. The pressure distribution across the valve disc was used with the known stiffness for calculating the displacement analytically. The new gap between the valve disc and the inlet was then updated. The flow model was then meshed again with the new geometry, readied for the next iteration. The iteration loop stopped, if the displacement difference reached a given convergence condition which was 10 nm in our analysis. On average, the coupled simulation stopped after three or four iterations. The simulation of our two-dimensional rotation-symmetric model with 14 848 elements required about 20 min on a Pentium IV personal computer with a clock frequency of 1.8 GHz. Figure 3 shows the simulated flow field in forward and backward directions. The numerical model is only used for fitting the measurement results in section 4 because of the constraints of an unknown exact elastic modulus of SU-8, an unknown initial gap, and the possible kipping movement of the valve disc.

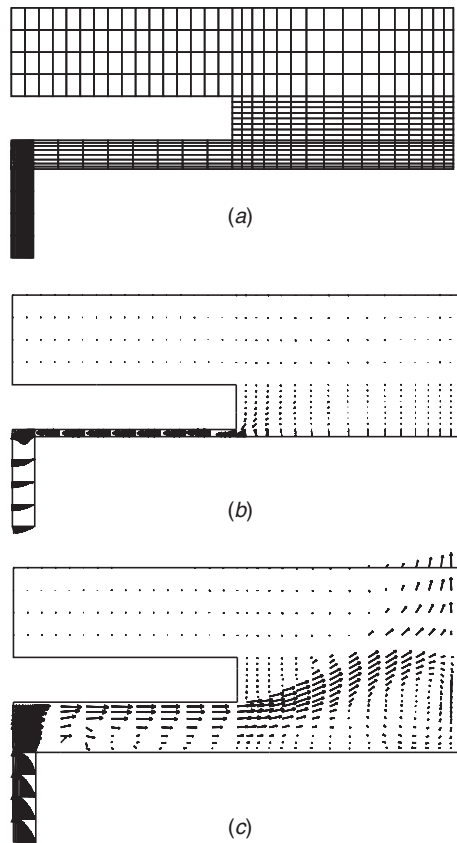


Figure 3. Semi-analytical coupled fluid-structural simulation of the microvalve: (a) grid model with the initial gap, (b) reverse direction, (c) forward direction (rotation-symmetric model; the velocity vectors in (b) and (c) are not to scale).

3. Fabrication

3.1. Polymeric surface micromachining with SU-8

The valves described above were fabricated in SU-8, a negative thick-film resist. We used SU-8 2100 (MicroChem, Corp, USA) for the fabrication of the 100 μm thick SU-8 layer. The SU-8 2000 family is a new formulation, which uses cyclopentanone (CP) as the solvent instead of γ -butyrolactone (GBL) in the standard SU-8 family.

The valve designs were first drawn with a CAD program and then printed on a polymer film with a high-resolution laser printer. The film was used as the lithography mask for the ultraviolet (UV) exposure of the SU-8 layer. The layers for inlet and outlet holes are placed on separate masks. This low-cost approach allows us to have a very short prototyping cycle. We developed a polymeric surface micromachining process with SU-8 as the functional layer. The process starts with cleaning a polished silicon wafer. The silicon wafer works as the handling substrate. A 100 nm chromium layer was sputtered on silicon (figure 4(a)). This chromium layer is the sacrificial layer for the later release of the SU-8 structures. SU-8 2100 was then spin-coated on the chromium layer. At a room temperature of 24 $^{\circ}\text{C}$, the spin speed was first ramped up in 5 s to 500 rpm. This speed remained constant for 5 s. The second ramp increased the speed from 500 to 2100 rpm in 10 s. The high speed was kept constant for 22 s. The final ramp

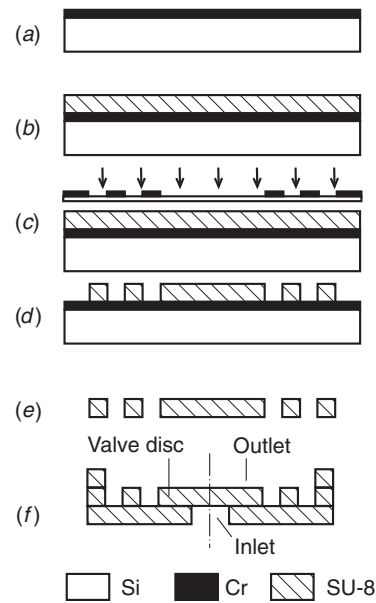


Figure 4. Fabrication process of SU-8 check valves using polymeric surface micromachining.

decreased the speed from 2100 rpm down to full stop in 20 s. This spin recipe results in a 100 μm thick SU-8 layer with a thickness variation of less than $\pm 2 \mu\text{m}$ (figure 4(b)).

A soft bake step follows the spin-coating step. Since SU-8 2100 still continues to reflow with a relatively low viscosity, care should be taken in levelling the wafer. The soft bake step was carried out in a convection oven. The wafer was kept at 65 $^{\circ}\text{C}$ for 10 min and then at 95 $^{\circ}\text{C}$ for 40 min. The wafer was then allowed to cool to room temperature before the UV exposure. The SU-8 layer was then exposed with an energy density of 525 mJ cm^{-2} using near-UV wavelengths. The polymer mask described above was used for this step (figure 4(c)).

Following the exposure step, another bake process allows SU-8 to polymerize further. The wafer with the exposed SU-8 layer was baked at 65 $^{\circ}\text{C}$ for 5 min and then at 95 $^{\circ}\text{C}$ for 10 min. The wafer was allowed to cool slowly in the switched-off oven to room temperature. This cooling step is crucial for avoiding microcracks and curling of the SU-8 film after release. SU-8 was then developed in propylene glycol methyl ether acetate (PGMEA; figure 4(d)). After cleaning with isopropyl alcohol (IPA), the wafer was blown dry with nitrogen. In the final step, chromium was etched away releasing the SU-8 layer (figure 3(e)). Figure 5 shows the fabricated micro check valves. The SU-8 structures were coated with a thin aluminium layer for the measurement with scanning electron microscopy (SEM).

3.2. Device assembly and packaging

Figure 4 describes the assembly of a stand-alone micro check valve with three SU-8 layers: the outlet layer, the valve layer and the inlet layer. Each layer has a form of a disc with a diameter of 5.5 mm. The inlet has a diameter of 100 μm , which is entirely covered by the valve disc (figure 6(a)). The outlet has a diameter of 2 mm (figure 6(b)), which is equal to

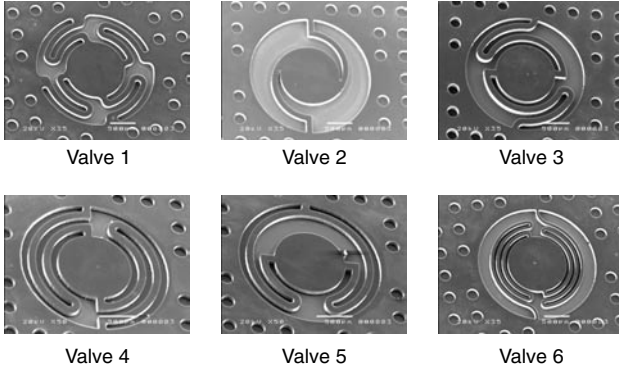


Figure 5. Fabricated SU-8 check valves.

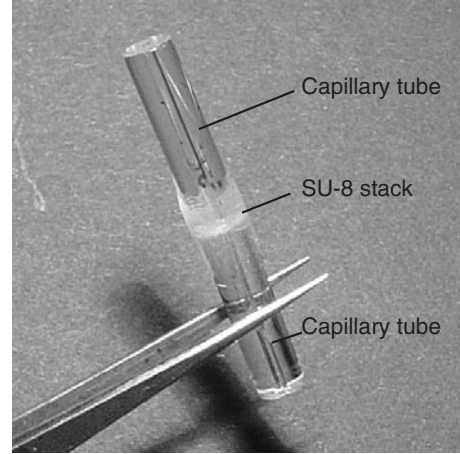
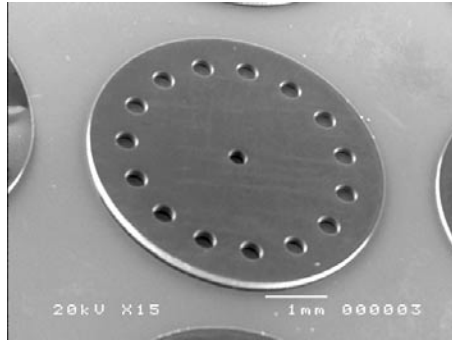
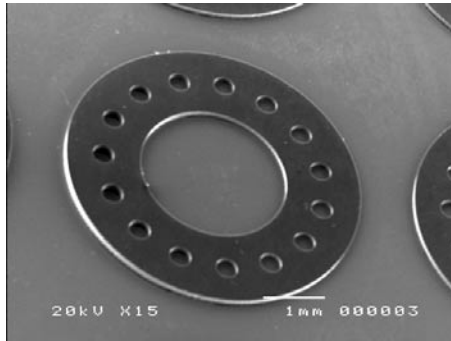


Figure 7. The assembled valve.



(a)



(b)

Figure 6. The inlet (a) and outlet (b) layers.

the opening diameter of the valve layer (figure 5). This three-layer design allows a maximum deflection of $100\ \mu\text{m}$ of the valve disc. Thus, the stress in the beams is kept at a relatively low value, which improves the fatigue life of the valve. In a micropump application [21] valve number 1 can withstand a few million deflection cycles.

The three-layer stack is pressed between two capillary tubes with an outer diameter of 5.5 mm and an inner diameter of 2 mm by a spanner. Epoxy glue was then applied around the tubes. After the glue was hardened, the device was released from the spanner readied for testing. Figure 7 shows the picture of one of the assembled valves.

4. Characterization results

The flow rectification behaviour of the check valves was tested with deionized (DI) water. The flow characteristics of the stand-alone valves was taken by measuring the pressure drop across the valve and the volumetric flow rate. The volumetric flow rate is determined by the travel speed of the water/air interface in a capillary with a known diameter. A large reservoir with different heights of the water surface emulates the inlet pressure and eliminates the error of height change during the measurement.

The pressure drop was measured with a differential pressure sensor (Honeywell 22PC-Series, $\pm 1\ \text{psi}$) which was calibrated for a pressure range from 0 to 6000 Pa.

The outlet of the valve was connected to a horizontal capillary with an inner diameter of 0.8 mm. The travel speed of the meniscus was determined by measuring the travel time over a fixed distance and converted into flow rate. The measurement error can be estimated by

$$\Delta \dot{Q} = \sqrt{\left(\frac{\Delta V}{t}\right)^2 + \left(\Delta t \frac{V}{t^2}\right)^2} \quad (7)$$

where V and t are the measured volume and time, and ΔV and Δt are the worst-case errors of the measurement. An error of less than 5% can be estimated for our measurement.

Figure 8 shows the results of the valves discussed in this paper. The results of the numerical model described in section 2 are used as the fitting curve for the measurement. The parameters of the numerical models, the spring constant k and the initial gap g_0 are given in the figure caption. It is obvious that due to the lower spring constant the valves with only 1 and 2 suspension arms allow higher flow rate in forward direction. However, they have large leakage flow rates in the reverse direction. This behaviour may be caused by the tipping movement of the valve disc. Even a small particle or assembly misalignment may cause a large gap due to this tipping movement. The model of an initial gap and a parallel disc movement is not ideal for this case.

Valve 1 shows almost no leakage due to the tight closure with four suspension arms. A tipping movement is not possible with the ortho-planar design. Thus, almost zero leakage can be achieved. The drawback is the stiff spring,

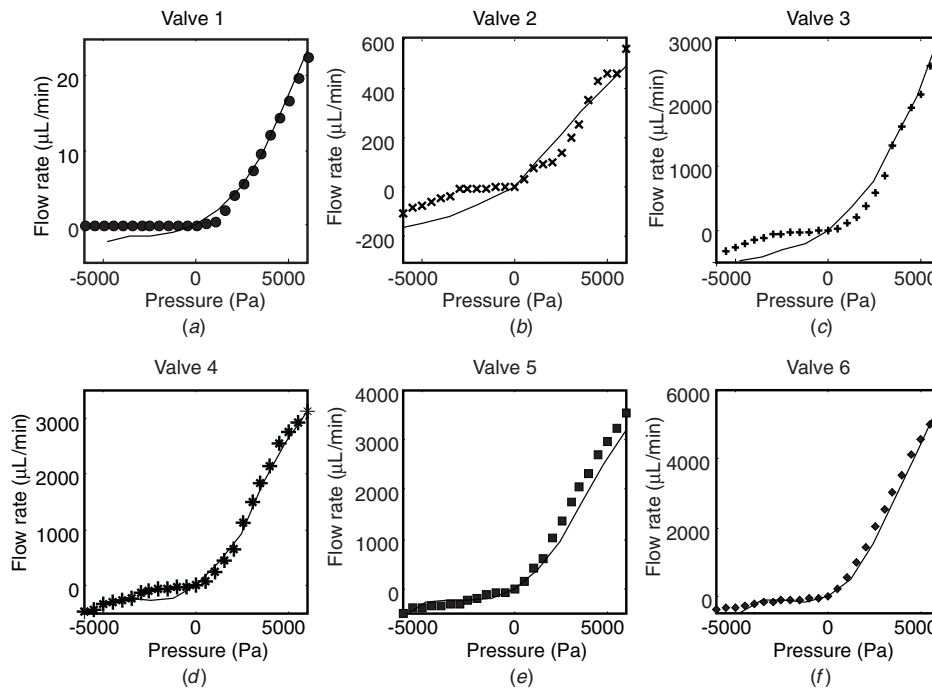


Figure 8. Measured flow behaviour of each microvalve and its fitting curve from the numerical model: (a) valve 1 ($k = 613 \text{ N m}^{-1}$, $g_0 = 9 \mu\text{m}$); (b) valve 2 ($k = 499 \text{ N m}^{-1}$, $g_0 = 50 \mu\text{m}$); (c) valve 3 ($k = 95 \text{ N m}^{-1}$, $g_0 = 65 \mu\text{m}$); (d) valve 4 ($k = 65 \text{ N m}^{-1}$, $g_0 = 60 \mu\text{m}$); (e) valve 5 ($k = 59 \text{ N m}^{-1}$, $g_0 = 65 \mu\text{m}$); (f) valve 6 ($k = 31 \text{ N m}^{-1}$, $g_0 = 65 \mu\text{m}$).

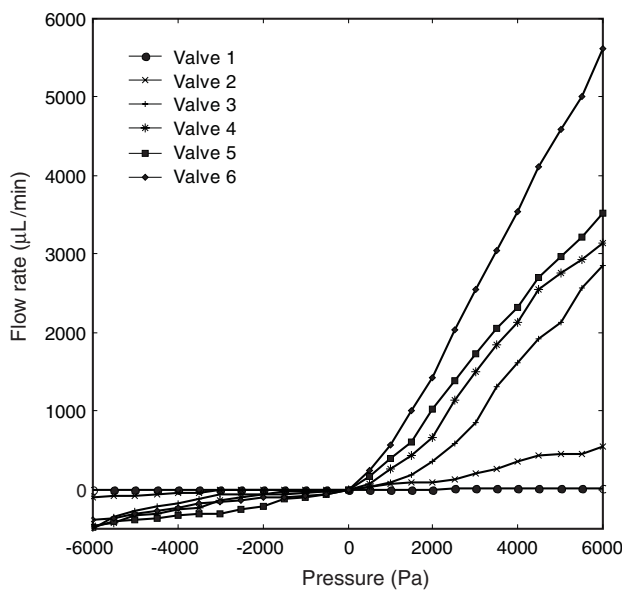


Figure 9. Flow characteristics of the stand-alone SU-8 micro check valves.

which causes very small flow rates in the forward direction (figure 8(a)).

Figure 9 compares the flow characteristics of all the valves.

5. Conclusions

Different micro check valves have been designed, fabricated in SU-8 and tested for functionality. The results show the feasibility of making a microfluidic system entirely of

polymeric material. The check valves have a clear rectification behaviour and can be opened with a relatively low inlet pressure of less than 1 kPa. Ortho-planar designs have shown better sealing characteristics due to the parallel out-of-plane motion. Valve designs with one and two suspension arms have large leakage flows, which are probably caused by the tipping motion of the valve discs. Valve design 1 was successfully used in a micropump, which can deliver up to 1 mL min^{-1} water flow and a back pressure of 2 kPa. The results of the pump will be reported in a separate paper [21]. The successful operation of the micro check valves and the pump indicate that our polymeric technology is relevant for low-cost mass fabrication of polymeric microfluidic cartridges. We are continuing efforts to design a low-cost, disposable cartridge for analytical chemistry. Only passive components such as micro check valves, micromixers, microchannels and pump chambers are integrated in the cartridge. Actuators are placed on the external evaluation device.

Acknowledgments

This work was supported by the academic research fund of the Ministry of Education Singapore, contract number RG11/02. The authors thank the students and staff of the Microlab, Singapore Polytechnic, for their collaboration and assistance during this project.

References

- [1] Nguyen N T and Wereley S T 2002 *Fundamentals and Applications of Microfluidics* (Boston: Artech House)
- [2] Paegel B M *et al* 2002 High throughput DNA sequencing with a microfabricated 96-lane capillary array electrophoresis bioprocessor *Proc. Natl. Acad. Sci.* **99** 254–579

- [3] Linder V *et al* 2002 Application of surface biopassivated disposable PDMS/glass chips to a heterogeneous competitive human serum IgG immunoassay with incorporated internal standard *Electrophoresis* **23** 740–9
- [4] Medintz I *et al* 2001 High-performance multiplex SNP analysis of three hemochromatosis-related mutations with capillary array electrophoresis microplates *Genome Res.* **11** 413–21
- [5] Anderson R C *et al* 2000 A miniature integrated device for automated multistep genetic assays *Nucl. Acids Res.* **28** 60
- [6] <http://www.istat.com>
- [7] Taylor M T *et al* 2003 Simulation of microfluidic pumping in a genomic DNA blood-processing cassette *J. Micromech. Microeng.* **13** 201–8
- [8] Tamanaha C R, Whitman L J and Colton R J 2002 *J. Micromech. Microeng.* **12** N7–N17
- [9] Grover W H *et al* 2003 Monolithic membrane valves and diaphragm pumps for practical large-scale integration into glass microfluidic devices *Sensors Actuators B* **89** 315–23
- [10] Krulevitch P *et al* 2002 Polymer-based packaging platform for hybrid microfluidic systems *Biomed. Microdevices* **4** 301–8
- [11] Shoji S and Esashi M 1990 Microflow devices and systems *J. Micromech. Microeng.* **4** 157–71
- [12] Nguyen N T, Huang X Y and Toh K C 2002 MEMS–micropumps: a review *ASME Trans., J. Fluids Eng.* **124** 384–92
- [13] Rapp R *et al* 1994 LIGA micropump for gases and liquids *Sensors Actuators A* **40** 57–61
- [14] Schomburg W K *et al* 1994 Microfluidic components in LIGA technique *J. Micromech. Microeng.* **4** 186–91
- [15] Boehm S, Olthuis W and Bergveld P 1999 A plastic micropump constructed with conventional techniques and materials *Sensors Actuators A* **77** 223–8
- [16] Howell L L 2001 *Compliant Mechanisms* (New York: Wiley)
- [17] Parise J J, Howell L L and Magleby S P 2001 Ortho-planar linear-motion springs *Mech. Mach. Theory* **36** 1281–99
- [18] Lorenz H *et al* 1997 SU-8: a low-cost negative resist for MEMS *J. Micromech. Microeng.* **7** 121–4
- [19] Ulrich J and Zengerle R 1996 Static and dynamic flow simulation of a KOH-etched microvalve using the finite-element method *Sensors Actuators A* **53** 379–85
- [20] Koch M, Evan A G R and Brunnschweiler A 1995 Coupled FEM simulation for the characterization of the fluid flow within a micromachined cantilever valve *Proc. Micromechanics Europe (Copenhagen)* pp 160–3
- [21] Nguyen N T and Truong T Q 2003 A fully polymeric micropump with piezoelectric actuator *Sensors Actuators B* at press